

STELLAR GALACTIC POPULATION CHARACTERIZATION USING GAIA PHOTOMETRY

J.M. Carrasco, C. Jordi, F. Figueras, J. Torra

Dept. Astronomia i Meteorologia, Universitat de Barcelona, Avda. Diagonal 647, E-08028 Barcelona, Spain

ABSTRACT

The spectroscopic features to be measured, their dependence as a function of T_{eff} , $\log g$ or $[M/H]$ for the various types of stars leading us to the design of the medium pass-bands, central wavelength and their blue and red limits are described. The design particularly accounts for the scientific key targets for the study of the origin and history of our Galaxy. This paper focusses on the Geneva-Barcelona medium-band photometric system.

Key words: Gaia; Photometry; Filter definition; Astrophysical parameters.

1. INTRODUCTION

The Gaia mission must provide the physical properties (T_{eff} , luminosity, chemical composition, peculiarities, anomalies, etc), with an accuracy sufficient for the quantitative description of the chemical and dynamical evolution of the Galaxy over all galactocentric distances.

The bands proposed by the Geneva-Barcelona team for the Gaia mission (Grenon et al. 1999a, 1999b, Jordi et al. 2003, 2004), are a compromise to have at the same time a performing classification tool for early, intermediate and late type stars up to the G -limiting magnitude. This performance was achieved by adopting bandwidths as broad as possible, without significant degradation of the physical information. We took special care to assure that abundances, gravities and temperatures at the needed accuracy could be derived for the scientific goals (ESA 2000).

For the optimization of the bands, synthetic photometry was realized using ATLAS9 (Kurucz 1991, 1994), BaSeL-2.2 (Lejeune et al. 1998) and PHOENIX team (Hauschildt et al. 1999, Allard et al. 2001) stellar atmosphere models.

Presently, this system is being optimized for the reddening determination and tested for possible improvements of chemical abundances determination by learning from other medium-band proposals for Gaia (Vansevicius 2004, Knude & Høg 2004, Straizys 2004). See Jordi &

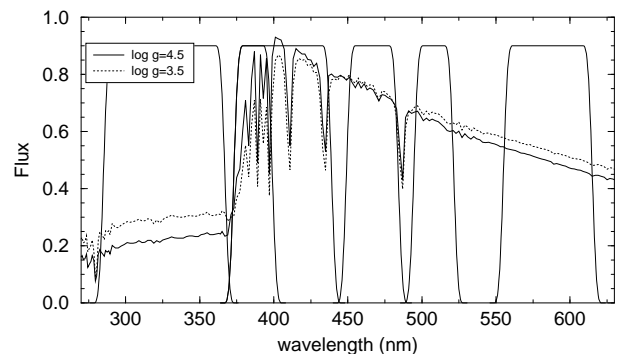


Figure 1. Kurucz's models for a A3-type star ($T_{\text{eff}} \sim 8500\text{K}$, with different surface gravities). Thin solid curves are the band-passes. The colour C_{33-41} versus a T_{eff} indicator, like C_{47-59} , is a measure of the Balmer jump (see Figure 5 left).

Høg (2005), for a detailed discussion of photometric system performances evaluation.

2. THE GAIA PHOTOMETRY

The UV domain contains the most useful information on gravity for early-type stars (see Figure 1) and on metallicity for F, G, K stars (see Figure 2 and Cayrel et al. 1999). In spectra of early-type stars, the Balmer continuum is devoid of absorption features. In ground-based photometry, the U band is naturally limited on the UV-C side, by saturated terrestrial O_3 bands. In space the F_{33} band should extend to the QE-CCD limit. This improves the determination of $[M/H]$ for G and K stars because of the presence of very many atomic lines. Any overlap of F_{33} with the Balmer jump would result in a loss of sensitivity to gravity for B and A stars.

The F_{41} filter is designed to measure Balmer lines for late B and A type stars, in the range from the Balmer jump up to H_γ , see again Figure 1. For F-type stars and cooler, the F_{41} filter measures the break short of 430 nm, due to a strong concentration of atomic and molecular lines, see Figure 2. In addition, the F_{41} band contains CN bands, strong CaII lines, the Q and R branches of CH radical and the P branch, less intense. When the abundance of

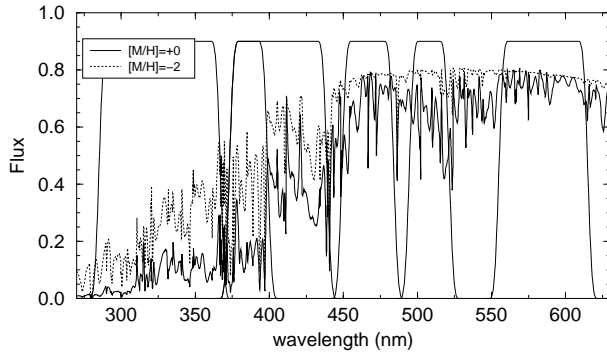


Figure 2. PHOENIX's models for a K2 V star ($T_{\text{eff}} \sim 5000\text{K}$, $\log g \sim 4.5$) with different metallicities. Thin solid curves are the band-passes. The line blocking in the UV regions is larger than in the violet domain. The colour C_{33-47} is a good indicator of metallicity (Cayrel et al. 1999).

CN increases the abundance of CH decreases, thus the flux measured in the F_{41} bandpass remains a very good indicator of the global metallicity. The F_{39} filter is introduced to better isolate CH from CN.

The F_{47} filter measures a domain where the absorption by atomic and molecular lines is minimum, see Figure 2. The flux in that domain corresponds to a pseudo-continuum, used with the F_{59} or F_{75} fluxes to derive T_{eff} . The blue side was defined to avoid certain CH contamination. With a red limit at 484 nm, the perturbation by H_{β} at 481 nm is small. This red limit is also imposed by the presence of the MgH band in particular for K dwarfs.

The F_{51} filter was designed to measure the complex MgH+Mg b, which is the best gravity indicator for late G to early M stars. It must be investigated if this band can be used to derive α -elements abundances.

The F_{59} band measures a pseudo-continuum with very low absorption by metallic lines, except by Na D which becomes very strong in SMR stars. F_{59} is limited on the blue side by the numerous metallic lines and on the red side by that of a strong TiO band. The cut at 615 nm avoids an excessive contamination by the TiO γ ' system bands. For stars later than K4, the F_{59} band becomes contaminated by TiO.

In very metal-poor low-luminosity dwarfs, the MgH band remains strong whereas TiO bands vanish completely. Red colours, low TiO and strong MgH are typical signatures of halo counterparts of M dwarfs.

The original purpose of the F_{65} band was the detection (when present) of emission features in the spectrum, thus allowing to detect peculiar objects (such as Be stars, T-Tau stars, etc). The band width (653–659 nm) was chosen for the detection of both H_{α} and [N I] 655/658 nm even in high-radial velocity stars. Since the strength of the line is sensible to effective temperature for early type stars, this band combined with a broad band centred at the same effective wavelength may provide an almost reddening-free index. This option is under investigation.

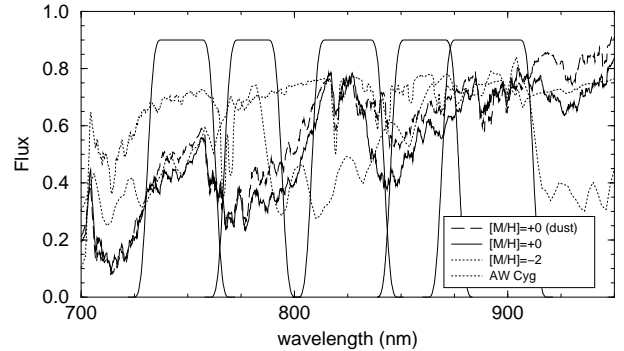


Figure 3. PHOENIX's models for a M5 V star ($T_{\text{eff}} \sim 3000\text{K}$, $\log g \sim 4.5$) with different metallicities. Solid line curves represent the bandpasses. The spectra of the C-star AW Cyg was taken from Gunn & Stryker (1983). The F_{75} and F_{89} bandpasses measure the continuum, while F_{78} measures the TiO band intensity and the F_{83} the CN depression.

The red bands (F_{75} , F_{78} , F_{83} , F_{89}) are designed to measure the temperature, the TiO and the CN abundance of red stars with T_{eff} below 4200 K.

F_{75} measures a portion of the spectrum where the absorption by TiO bands is minimum, see Figure 3. The second point of pseudo-continuum is measured by the F_{89} filter. In spectra of B, A, F stars, the F_{89} band measures the Paschen jump and lines, whereas the continuum is measured by F_{75} , F_{78} and F_{83} bands.

A band as red as possible improves the reddening determination of intermediate stars (Vansévičius & Bridzius, 2002). We are currently studying which of our pseudo-continuum bands in the red domain can be suppressed and substituted by this extremely red one. A band in that domain would also improve the performance of the photometric system for the Solar System objects taxonomy.

As expected, the measurement of the Paschen jump is delicate for A-type stars because of its small amplitude. The gravity effect is limited to about 0.18 mag when main sequence stars are compared to luminous giants while Balmer's jump provides a change of ~ 0.8 mag.

The F_{83} band is designed to measure either the continuum bluewards of the Paschen jump wavelength, or a strong CN band for R, N, C stars (compare the spectrum of AW Cyg in Figure 3 with the non-C stars). For M stars, F_{83} measures a spectral domain with weak absorption by TiO. The blue side was fixed to avoid VO band that develops from \sim M5-type stars.

The distinction between M and C stars is realized with the F_{75} , F_{78} , F_{83} and F_{89} bands (see again Figure 3). At a given temperature, the fluxes are similar in the F_{78} and F_{89} for O-rich stars (the M sequence) and for C-rich stars (the C sequence), but very different in the F_{75} and F_{83} bands, namely because of strong CN bands. The separation between M and C stars is indeed possible even if they are heavily reddened.

Finally, the F_{86} band covers the wavelength range of the

RVS spectrometer. This passband is important for classification of heavily reddened early-type stars, when they are too faint to be well measured in the ultraviolet.

3. DERIVATION OF ASTROPHYSICAL PARAMETERS

3.1. Luminosity Determination

The MgH+Mg b band intensity is nearly invariant as a function of [M/H] for G and K dwarfs and subgiants. This behaviour allows to separate luminosities down to the G -limiting magnitude (see Figure 4), especially in the Galactic poles direction. Its intensity reaches a maximum around K7V. It is also useful to discriminate between M dwarfs and cool white dwarfs.

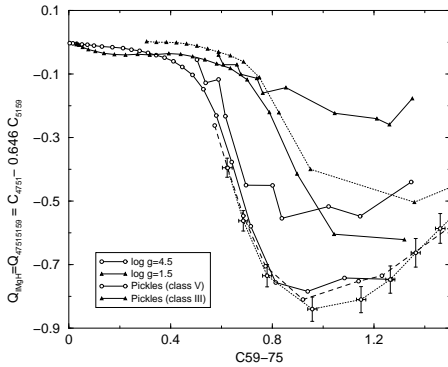


Figure 4. Reddening-free $Q_{I_{Mg}}$ derived from Kurucz's (thin solid lines) and PHOENIX's (without dust: thin dotted lines; with dust: dashed lines) theoretical models for stars with solar metallicity, as well as for empirical (thick solid lines) spectra (Pickles 1998). Error bars correspond to $G = 19$ mag at the end of the mission.

The Balmer jump, measured by C_{33-41} versus T_{eff} (Figure 5 left), also helps with the determination of luminosity. The amplitude of variation is of ~ 0.8 mag for a $\log g$ change from 4.5 to 1.5 leading to accurate estimates of $\log g$ down to $G = 19$ ($\sigma_{\log g} \approx 0.05$ dex).

We also have to take into account the valuable information coming from the extremely accurate trigonometric parallax, that will provide a direct determination of luminosity for many of the observed stars.

3.2. Abundance Determination

Figure 5 (right) demonstrates the capability of the F_{41} band to derive global abundances through the reddening-free parameter $Q_{I_z} = Q_{41477889}$. The errors of Q_{I_z} slightly decrease with C_{59-75} while the sensitivity to [M/H] increases. A good metallicity discrimination ($\sigma_{[M/H]} < 0.1$ dex) may be obtained down to $V \sim 18$ for typical red giants. $\sigma_{[M/H]} \approx 0.17$ dex for a star of 4200K and $G = 19$ ($G - V \sim -0.14$). Even, the metallicities

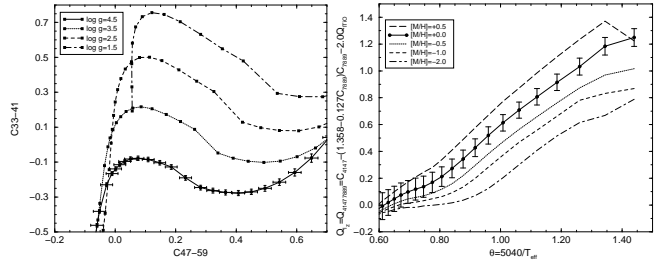


Figure 5. Left: The Balmer jump as measured by the C_{33-41} index for solar metallicity stars. Error bars correspond to $G = 19$ mag at the end of the mission. Right: Reddening-free index $Q_{I_z} = Q_{41477889}$ for stars with $\log g = 3$ vs. θ for different metallicities using PHOENIX models. Error bars give the errors for a $G = 19$ star at the end of the mission.

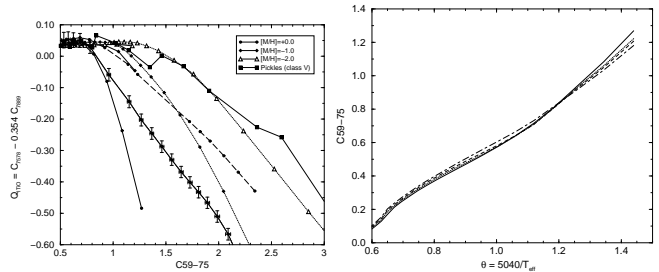


Figure 6. Left: Reddening-free $Q_{I_{TiO}}$ derived using Kurucz's models (thin solid lines), PHOENIX models (without dust: dotted lines; with dust: dashed line) and from empirical spectra (thick solid line, Pickles 1998) for dwarfs. Different symbols mean different metal abundances. Error bars correspond to a star of $G = 19$ at the end of the mission. Right: The C_{59-75} colour and its correlation with reciprocal temperature θ for dwarf stars of several metallicities.

for the horizontal branch stars of the LMC ($V \approx 20$) will be accessible.

An analogous reddening-free index $Q_{39477889}$ is also suitable, although the estimated error is larger.

Figure 6 (left) shows the reddening-free $Q_{I_{TiO}}$ as a function of T_{eff} . The $Q_{I_{TiO}}$ measures the TiO band intensity around 780 nm, relative to the F_{75} and F_{89} pseudo-continua. For late K and M dwarfs, I_{TiO} shows a strong dependence on [M/H], allowing a precise determination of [Ti/H]. The figure shows that although the PHOENIX models predict a thinner range of $Q_{I_{TiO}}$ values than Kurucz's models, this index is still providing astrophysical information down to low temperatures ($C_{59-75} \sim 3$ corresponds to $T_{\text{eff}} \sim 2500$ K). Thus, the $Q_{I_{TiO}}$ allows an easy separation of SMRs, old and thick disc stars. Estimated uncertainties using Kurucz and PHOENIX SEDs differ in 0.05 dex and 0.08 dex at $V = 18$ and 20 mag, respectively.

[Ti/H] may be defined with $\sigma_{[Ti/H]} < 0.1$ dex, down to $V = 18.5$ or 20, depending on the models, for M dwarfs with $T_{\text{eff}} = 3500$ K, see Figure 6 right. Even with the less favourable predictions given by PHOENIX models,

$\sigma_{[Ti/H]}$ is ± 0.075 dex at $V = 18$, i.e. $G \sim 16.5$, sufficient enough to identify moving group members. It is still possible to distinguish thin and thick disc M2–M3 dwarfs at the G -limiting magnitude.

3.3. Temperature Determination

The colour indices sensitive mainly to T_{eff} , are almost linear functions of the reciprocal temperature $\theta = 5040/T_{\text{eff}}$. It is why colour indices will be plotted versus θ rather than T_{eff} . For stars cooler than 10 000K, metallicity effects on the colours are function of $[M/H]$, T_{eff} and $\log g$. C_{59-75} is the temperature estimator, by far the less sensitive to $[M/H]$ for dwarfs in the range 10 000 to 3500 K, as shown in Figure 6 (right).

The colour index C_{47-59} shows metallicity residuals, growing with decreasing T_{eff} . These residuals are still acceptable for A, F, G dwarfs, because they are brighter in F_{59} band than in F_{75} band, and also because C_{47-59} is less sensitive to reddening than C_{59-75} . A slight contamination by TiO is noticeable for $\theta > 1.25$ ($T_{\text{eff}} < 4000\text{K}$).

For M stars and cooler, C_{75-89} is the best temperature estimate. Although not fully independent on $[M/H]$, it shows a monotonic growth with θ . It could be corrected for $[M/H]$ through the TiO index described below, although this step is not a must since iso- $[M/H]$ and iso- T_{eff} lines will be drawn in the colour-colour diagrams.

The errors on temperature are dependent on the stars colours and apparent magnitude. An excellent T_{eff} estimation with $\sigma_{T_{\text{eff}}} < 50\text{K}$ (1.4%) is obtained down to $V = 20$ when C_{59-75} and C_{75-89} indices are used for the M dwarf, the second being more precise below 3500 K and so, suitable for cool M dwarfs and brown dwarfs.

For solar type stars, the accuracy on T_{eff} is slightly better when the C_{47-59} index is used rather than C_{59-75} index, although more sensitive to reddening. The threshold $\sigma_{T_{\text{eff}}} = 100\text{K}$ (1.7%) is reached for $V = 19$. When ages are determined from turn-off temperatures alone, 100 K error leads to errors on the age up to 2 Gyr at age = 10–14 Gyr.

4. FUTURE DEVELOPMENT

Our immediate goal is to improve the present proposal of this MBP system still on the basis of scientific key targets in collaboration with the other members of the Photometry Working Group, studying how the different $[\alpha/\text{Fe}]$ abundances (variable with galactocentric distance and metal content) or the violet CNO anomalies may affect the global metallicity determination. The performance of the system for those type of stars not yet considered (WR, with H_{α} emission, Be, S, flare, white dwarfs, T-Tauri, metal-deficient M dwarfs, ...) and non-stellar objects (QSO, Solar System objects, ...) will be evaluated.

ACKNOWLEDGMENTS

The authors specially thank M. Grenon, who provided his deep knowledge to build the basis of this system. This work has been supported by the MCYT under contract PNE2003-04352.

REFERENCES

- Allard F., Hauschildt, P.H., Alexander, D.R., Tamanai, A., Schweitzer, A., 2001 ApJ, 556, 357
- Cardelli J.A., Clayton G.C., Mathis J.S., 1989 ApJ, 345, 245
- Cayrel R., Castelli F., Cav't Verr C., 1999 *Atelier GAIA: L'astrométrie pour l'astrophysique et l'astrodynamique*, M. Froeschlé, F. Mignard, eds., Observatoire de la Côte d'Azur
- ESA, 2000 *GAIA, Concept and Technology Study Report*, ESA-SCI(2000)4
- Grenon M., Jordi C., Figueras F., Torra J., 1999a, Gaia technical report MGUB-PWG-002
- Grenon M., Jordi C., Figueras F., Torra J., 1999b, Gaia technical report MGUB-PWG-003
- Gunn F.E., Stryker L.L., 1983 ApJS, 52, 121
- Hauschildt P.H., Allard F., Baron E. 1999 ApJ, 512, 377
- Jordi, C., Grenon, M., Figueras, F., Torra, J., Carrasco, J.M., 2003, Gaia technical report UB-PWG-011
- Jordi, C., Figueras, F., Torra, J., Carrasco, J.M., 2004, Gaia technical report UB-PWG-016
- Jordi, C., Høg, E., 2005, ESA SP-576, this volume
- Knude, J., Høg, E., 2004, Gaia technical report GAIA-CUO-148
- Kurucz R.L., 1991 in *Precision Photometry: Astrophysics of the Galaxy*, A.G.D. Philip, A.R. Uppgren, K.A. Janes, eds., L. Davis Press, Schenectady, p. 27
- Kurucz R.L., 1994 CD-ROM No 19
- Lejeune, T., F. Cuisinier, F., Buser, R., 1998 *A standard stellar library for evolutionary synthesis. II. The M dwarf extension*, A & A Suppl. Ser., 130, 65-75
- Pickles A.J., 1998 PASP 110, 863
- Straizys, V., 2004, Gaia technical report GAIA-VILN-003
- Vansevicius, V., 2004, Gaia technical report GAIA-VIL-014
- Vansevicius, V., Bridzius, A., 2002, *Gaia photometric performances*, U. Munari, ed., ASP Conf. Ser. Vol 298, p. 41-50